IMAGE AUTHENTICATION THROUGH Z-TRANSFORM WITH LOW ENERGY AND BANDWIDTH (IAZT)

Madhumita Sengupta[1] and J. K. Mandal[2]

Department of Computer Science and Engineering,University of Kalyani, Kalyani, Nadia, Pin. 741235, West Bengal, India

ABSTRACT

In this paper a Z-transform based image authentication technique termed as IAZT has been proposed to authenticate gray scale images. The technique uses energy efficient and low bandwidth based invisible data embedding with a minimal computational complexity. Near about half of the bandwidth is required compared to the traditional Z–transform while transmitting the multimedia contents such as images with authenticating message through network. This authenticating technique may be used for copyright protection or ownership verification. Experimental results are computed and compared with the existing authentication techniques like Li's method [11], SCDFT [13], Region-Based method [14] and many more based on Mean Square Error (MSE), Peak Signal to Noise Ratio (PSNR), Image Fidelity (IF), Universal Quality Image (UQI) and Structural Similarity Index Measurement (SSIM) which shows better performance in IAZT.

KEYWORDS

Z-Transform; Frequency Domain; Watermarking; Mean Square Error (MSE); Peak Signal to Noise Ratio (PSNR); Image Fidelity (IF); Universal Quality Image (UQI); Structural Similarity Index Measurement (SSIM).

1. INTRODUCTION

In today's digital world there is an enormous increase in the amount of multimedia content over internet such as image, video and audio materials. Such materials are traverse through wire and unwired medium in a carryon fashion.

Small digital device such as tablet, capsule, mobile, PDA's and many others are not yet small in physical senses due to their processing power and memory capacity. But the problem of sharing vast amount of multimedia contents over internet creates a concern among researchers regarding the bandwidth utilization. In case of static spectrum assignment for mobile or radio networks bandwidth becomes a major concern. Digital devices may improve their performance by improving processor or memory unit but bandwidth becomes the major limitation for transferring huge digital data.

In case of gray scale images each element called pixel, representing the luminance at a given point in the image commonly represented by an 8 bit number in a spatial domain. Digital data traverse through network in a bit form of spatial data or frequency components. A single flip of bit is enough to destroy single pixel, but in case of frequency domain signal/images are first

DOI : 10.5121/ijnsa.2013.5504

converted from spatial domain. Thus the probability of pixel value changes decreases as compared to spatial domain.

Many transformation techniques such as DFT[1], DCT[2,9,10], DWT[3], Daubechies[15] and others are already implemented in digital world and widely used in steganography[4], data compression and many more.

This paper proposed a frequency domain based technique where the digital content such as image is converted form spatial domain to Z-domain with a 2x2 sliding window based mask in a row major order to generate 2x2 real value and 2x2 imaginary value with less amount of computation and without the trigonometry complexity. This paper also emphasis on transmitting the image over unsecure network with detection of tempering through invisible watermarking, where half of the Z domain coefficients are enough to regenerate original image and find out the damaged portion.

Various parametric tests are performed and results obtained are compared with most recent existing techniques such as, WTSIC [5], Yuancheng Li's Method [11] and Region-Based watermarking [14], based on Mean Square Error (MSE), Peak Signal to Noise Ratio (PSNR), Image Fidelity (IF) analysis [7] and Universal Quality Image (UQI) and Structural Similarity Index Measurement (SSIM) [17] which shows a consistent relationship with the existing techniques.

Section 2 of this paper deals with the technique with six sub sections. Results and discussions are outlined in section 3, conclusions are drawn in section 4 and references are given at end.

2. THE TECHNIQUE

The IAZT technique is divided into four major tasks. Forward Z-transform as describe in section 2.1, Inverse Z-Transform given in section 2.2, 2.5 elaborate the procedure of bandwidth minimization and 2.6 emphases on embedding technique. Traditional and fast Z-transform calculations are also done with example in section 2.3 and 2.4 respectively.

2.1. Forward Z-Transformation

Z-transform in signal processing converts a discrete time domain signal which is a sequence of real or complex numbers into a complex frequency domain representation. Z-transform can be defined in two ways, unilaterally or bilaterally.

In bilateral or two sided Z-transform of discrete time signal x[n] is the formal power series $X(z)$ defined by eq(1).

$$X(z) = Z\{x[n]\} = \sum_{n=-\infty}^{\infty} x[n]z^{-n} \qquad (1)$$

Where n is an integer and z is, in general, a complex number.

Alternatively, in cases where x[n] is defined only for n ≥0, the single sided or unilateral Z-transform is defined by eq(2).

$$X(z) = Z\{x[n]\} = \sum_{n=0}^{\infty} x[n] z^{-n} \tag{2}$$
$$z = re^{j\omega} = r(\cos\omega + j\sin\omega)$$

Where r is the magnitude of $X(z)$, j is the imaginary unit, and ω is the angle in radians. We get eq(3) by substituting the value of $X(z)$ in eq(2).

$$X(z) = Z\{x[n]\} = \sum_{n=0}^{\infty} x[n] r^{-n} e^{-j\omega n} \tag{3}$$
$$or \qquad X(z) = Z\{x[n]\} = \sum_{n=0}^{\infty} x[n] r^{-n} (\cos\omega + j\sin\omega)^{-n}$$

On applying eq(3) for forward transformation over 2x2 mask of cover image in a row major order, four frequency component generates such as lower, horizontal, vertical and complex conjugate pair of horizontal frequency as shown in figure 1.a this is similar to subband coding[5].

Every frequency coefficients in lower to higher frequency bands are complex number in the format of ‘a + *j* b’. Separation of real and imaginary parts is shown in figure 1.b and 1.c respectively.

Lower Frequency (LF)	*Horizontal frequency (HF)*
Vertical frequency (VF)	*Complex conjugate pair of (HF)*

(a) Z-coefficient quadrants of complex value ‘a + *j* b’

Real part of LF	*Real part of HF*
Real part of VF	*Real part of HF*

(b) Real part of all frequency components

Imaginary part of LF	*Imaginary part of HF*
Imaginary part of VF	*Negation of Imaginary part of HF*

(c) Imaginary part of all frequency components

Figure. 1. Structural representation of forward Z-Transform (FZT)

2.2. Inverse Z-Transformation

Every transform technique exists with pair of equation, forward and inverse. The inverse Z-transform can be obtained by eq(4).

$$x[n] = Z^{-1}\{X(z)\} = \frac{1}{2\pi j} \oint_C X(z) z^{n-1}\, dz \tag{4}$$

where C is a counter clockwise closed path encircling the origin and entirely in the region of convergence (ROC). A special case of this contour integral occurs when C is the unit circle. The inverse Z-transform simplifies to eq (5).

$$x[n] = \frac{1}{2\pi} \int_{-\pi}^{+\pi} X(e^{j\omega})\, e^{j\omega n}\, d\omega \tag{5}$$

The original gray scale image as shown in figure 2.a 'Map.pgm' on forward Z transform (FZT) generates four real value subband and four imaginary subband as shown in figure 2.b and 2.d respectively. The information on the bands are emphasis through threshold as shown in figure 2.c and 2.e for real and imaginary parts respectively. Threshold increases the brightness of the small information present in the band as the value of frequency coefficients are not belonging to the range of image. Inverse Z transform applied on real and imaginary parts generate lossless image back with a MSE[7] as zero and that of PSNR[7] is infinity.

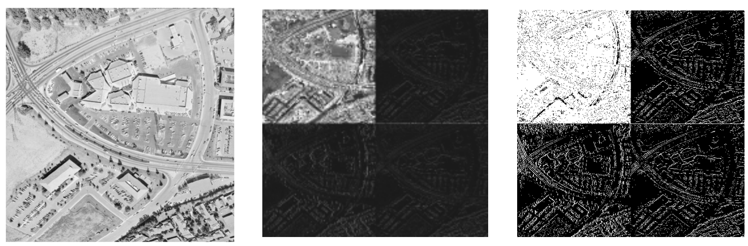

(a) Original Map (b) Real value after FZT (c) Threshold Real valued part

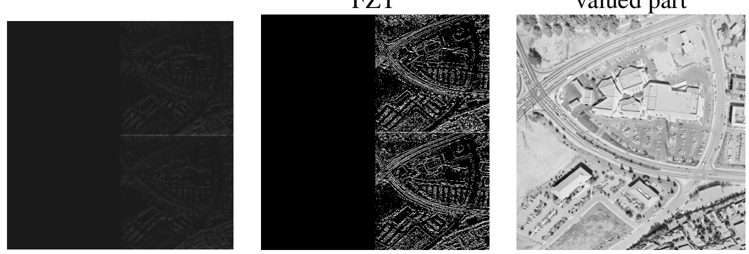

(d) Imaginary value after FZT (e) Threshold Imaginary part (f) Regeneration through inverse transform (IZT)

Figure. 2. Original image with Z domain coefficients, real and imaginary followed by inverse transform over coefficients

2.3. Traditional Z Transform

We have consider a special case of Z-transform where the value of r is taken as 1, and the angular frequency ω € {[0, π/2, π, 3π/2]}. The forward Z-transformation for the vector X (single mask of 2 x 2) is represented in figure 4(a), and the equation is given in eq (6). The elaborate form of eq (6) is shown in eq (7) where C_v is the coefficient value.

X_{00}	X_{01}
X_{10}	X_{11}

(a) Single mask

R_{00}	R_{01}
R_{10}	R_{11}

(b) Real value after FZT

I_{00}	I_{01}
I_{10}	I_{11}

(c) Imaginary value after FZT

Figure. 3. Single mask representation of Image and its components after forward Z-Transformation (FZT).

$$X(z) = Z\{x[n]\} = \sum_{n=0}^{3} x[n]r^{-n}(\cos\omega + j\sin\omega)^{-n} \tag{6}$$

$$C_v = [x[0]r^{-0}(\cos\omega + j\sin\omega)^{-0}] + [x[1]r^{-1}(\cos\omega + j\sin\omega)^{-1}] + [x[2]r^{-2}(\cos\omega + j\sin\omega)^{-2}] + [x[3]r^{-3}(\cos\omega + j\sin\omega)^{-3}] \tag{7}$$

Different angular frequency ω € {[0, $\pi/2$, π, $3\pi/2$]} is taken and with r = 1 the complex coefficients values $C_v = R_{lm} + jI_{lm}$ are calculated by equation set eq(8).

$$R_{lm} + jI_{lm} = \sum_{k=0}^{3}[x[k]1^{-k}(\cos\omega + \sin\omega)^{-k}] \tag{8}$$

Here ω depends on the value of lm.

$l \downarrow$ \ $m \rightarrow$	0	1
0	$\omega = 0$	$\omega = \pi/2$
1	$\omega = \pi$	$\omega = 3\pi/2$

Example 1:

Let's take vector X_{ij} = (146, 56, 118, 100); r = 1; and ω € {[0, 90, 180, 270]}. As per eq (8) calculation are followed and represented in figure 4.

$R_{00} + jI_{00} = [146 * 1^0 (\cos 0 + j\sin 0)^0] + [56 * 1^{-1} (\cos 0 + j\sin 0)^{-1}] + [118 * 1^{-2} (\cos 0 + j\sin 0)^{-2}] + [100 * 1^{-3} (\cos 0 + j\sin 0)^{-3}]$

$= [146 * (1 + j\,0)^0] + [56 * (1 + j\,0)^{-1}] + [118 * (1 + j\,0)^{-2}] + [100 * (1 + j\,0)^{-3}]$

$= [146 + 56 + 118 + 100] + j\,0 = 420 + 0\,j$

Likewise

$R_{01} + j\,I_{01} = 28 + j\,44$, $R_{10} + j\,I_{10} = 108 + j\,0$, $R_{11} + j\,I_{11} = 28 - j\,44$

(a) Single mask

146	56
118	100

(b) Real value after FZT

420	28
108	28

(c) Imaginary value after FZT

0	44
0	-44

Figure. 4. Example 1 represented with its components after FZT

2.4. Fast Z-Transformation

Z-Transform may also be represented with minimizing the computation and without the use of trigonometric functions, only by applying addition and subtraction. The frequency coefficients on FZT are complex numbers in the format of a + j b. The value of 'a' and 'b' on calculating by traditional Z transform are identical as calculated by Fast Z- transform. Fast Z transformation required less number of complex calculations as compared by traditional calculation.

2.4.1Algorithm for forward Z-transformation

Input: X_{00}, X_{01}, X_{10} and X_{11}.
Output: R_{00}, R_{01}, R_{10}, R_{11}, I_{00}, I_{01}, I_{10}, and I_{11}.
Method: Perform arithmetic calculation for fast forward Z-transform.
Step1: R_{00} and I_{00} calculation by eq (9)

$$R_{00} = \sum_{i,j=0}^{1} X_{ij} \tag{9}$$

$$R_{00} = (X_{00} + X_{01} + X_{10} + X_{11})$$

Step2: R_{10} and I_{10} calculation by eq(10)

$$R_{10} = \sum_{i=0}^{1} X_{i0} - \sum_{i=0}^{1} X_{i1} \tag{10}$$

$$R_{10} = (X_{00} + X_{10}) - (X_{01} + X_{11})$$

Step 3: R_{01} and I_{01} calculation by eq (11) and eq (12)

$$R_{01} + I_{01} = \sum_{i=0}^{1} X_{ii} - \sum_{i=0}^{1} X_{ii'} \tag{11}$$

$$R_{01} + I_{01} = (X_{00} + X_{11}) - (X_{01} + X_{10})$$

$$R_{01} - I_{01} = \sum_{i=0}^{1} X_{0i} - \sum_{i=0}^{1} X_{1i} \tag{12}$$

$$R_{01} - I_{01} = (X_{00} + X_{01}) - (X_{10} + X_{11})$$

Equation 11 shows a relation as $a*x + b*y = c_1$ and $a*x - b*y = c_2$, where 'a' and 'b' are depend on the value of r used. Two unknown x and y needs to be calculated by two equation11 and 12.
Step 4: R_{11} and I_{11} calculation by eq (13)

$$R_{11} = R_{01} \text{ and } I_{11} = -I_{01} \tag{13}$$

Let's recalculate the sample taken in example 1 with fast z-transform: -

$R_{00} = (146 + 56 + 118 + 100) = 420$
$R_{10} = (146+118) - (56 + 100) = 108$
$R_{01} + I_{01} = (146 + 100) - (56+118)$

$$R_{01} + I_{01} = 72 \tag{14}$$

$R_{01} - I_{01} = (146 + 56) - (118 + 100)$

$$R_{01} - I_{01} = -16 \tag{15}$$

There are two unknowns and two equations eq (14) and eq (15) by equating this two equations we can have the value of R_{01} and I_{01}. Such as follows, Eq (15) can rewritten as $R_{01} = -16 + I_{01,}$ that is when substituted in eq (14) we get, $-16 + 2I_{01} = 72$, that means, $2 I_{01} = 72 + 16$ or $I_{01} = 44$. When substituting $I_{01} = 44$, in eq (15) we achieved, $R_{01} = -16 + 44$, that is $R_{01} = 28$.

Thus, R_{01} = 28 and I_{01} = 44

Now R_{11} is equivalent to R_{01}, That is 28 and I_{11} is negation of I_{01}, which is -44 by eq (13). This two pair 28 + j 44 and 28 – j 44 are known as complex conjugate pair.

2.4.2 Algorithm for Inverse Z-Transformation

In case of inverse transform the calculation will is done using eq(16) to eq(19)
Input : $R_{(a)}$, $R_{(b)}$, $R_{(c)}$, $R_{(d)}$, $I_{(a)}$, $I_{(b)}$, $I_{(c)}$, and $I_{(d)}$.
Output: X_{00}, X_{01}, X_{10} and X_{11}.
Method: Perform arithmetic calculation by equation set (16) to (19) for fast inverse Z-transformation
Step1: Calculate X_{00} by eq (16).

$$X_{00} = \frac{1}{4}\sum_{i,j=0}^{1} R_{ij} + I_{ij} \tag{16}$$

Elaborated as:- $X_{00} = [\{(R_{00}+I_{00}) + (R_{01}+I_{01})\} + \{(R_{10}+I_{10}) + (R_{11}+I_{11})\}] / 4$
Step 2: Calculate X_{01} by eq (17).

$$X_{01} = \frac{1}{4}\left\{\sum_{i=0}^{1}(R_{ii} + I_{ii}) - \sum_{i=0}^{1}(R_{ii`} + I_{ii`})\right\} \tag{17}$$

Elaborated as:- $X_{01} = [\{(R_{00}+I_{00}) – (R_{01}+I_{01})\} – \{(R_{10}+I_{10}) – (R_{11}+I_{11})\}] / 4$
Step3: Calculate X_{10} by eq (18).

$$X_{10} = \frac{1}{4}\left\{\sum_{i=0}^{1}(R_{i0} + I_{i0}) - \sum_{i=0}^{1}(R_{i1} + I_{i1})\right\} \tag{18}$$

Elaborated as: - $X_{10} = [\{(R_{00}+I_{00}) – (R_{01}+I_{01})\} + \{(R_{10}+I_{10}) – (R_{11}+I_{11})\}] / 4$
Step4: Calculate X_{11} by eq (19).

$$X_{11} = \frac{1}{4}\left\{\sum_{i=0}^{1}(R_{0i} + I_{0i}) - \sum_{i=0}^{1}(R_{1i} + I_{1i})\right\} \tag{19}$$

Elaborated as: - $X_{11} = [\{(R_{00}+I_{00}) + (R_{01}+I_{01})\} – \{(R_{10}+I_{10}) + (R_{11}+I_{11})\}] / 4$

Calculation with sample value of example 1:

X_{00} = [{(420+ 0) + (28 + 44)} + {(108+ 0) + (28+ -44)}] / 4 = 146
X_{01} = [{(420+ 0) – (28 + 44)} – {(108+ 0) – (28+ -44)}] / 4 = 56
X_{10} = [{(420+ 0) – (28 + 44)} + {(108+ 0) – (28+ -44)}] / 4 = 118
X_{11} = [{(420+ 0) + (28 + 44)} – {(108+ 0) + (28+ -44)}] / 4 = 100

2.5. Bandwidth Minimization/Transmission Efficiency

A 2 x 2 mask of spatial data after FZT generates two 2 x 2 matrixes for real and imaginary frequency coefficient values, which means, information need to traverse after FZT will become double in terms of data. An examples is shown in figure 4 based on the representation of figure 3. On analysis of eight subbands, four real and four imaginary valued, based on the temporary environment created for z transform. It can be clearly elucidate that at most six subbands are required at destination to regenerate the lossless image, due to the entire zero value imaginary part for lower frequency (LF) and vertical frequency (VF) (in this case due to ω). Two more subbands can reduce without any loss due to the complex conjugate pair of horizontal frequency (HF). Thus in total, minimum requirement is four subbands out of eight to regenerate the original image without any loss as shown in figure 5. Few more examples are also shown in figure 9.

Figure. 5. Four subband required to generate the lossless image, Map image subbands to minimize bandwidth, real value of LF coefficients, real value of HF coefficients, real value of VF coefficient and Imaginary part of HF (Threshold Image).

2.6. Embedding Technique

On first level forward transformation in Z-domain the image is represented in eight sub image/bands [16] as shown in fig. 2(b) and 2(d). The subbands are tag by name shown in figure 1. In proposed IAZT only four bands [16] are declared as compulsory for regeneration of image on receiver side with secret invisible message/watermark as shown in figure 5. Out of four compulsory bands ‘real part of vertical frequency’, ‘real part of horizontal frequency’ and ‘Imaginary part of horizontal frequency’ may be used to embed secret information. The position of embedding bit is selected on the basis of hash function.

Embedding is based on payload, for 0.5 bpB of payload the ‘real part of vertical frequency’ is embedded by two secret bits per byte, results are shown in table 1. Same payload may be achieved by embedding two bits per byte in ‘real part of horizontal frequency’ and in ‘imaginary part of horizontal frequency’. Distortion calculation of original image with stego image is shown in table 2 and table 3 respectively. Payload may be enhanced by embedding three or four bits per byte in real or imaginary bands, to achieve 0.7 and 1.0 bpB, results are shown in table 4 to table 7 respectively. Table 8 shows the overall comparison between varies bands used for embedding, with different payloads.

2.6.1 Insertion

Bits are inserted based on a hash function where embedding position in frequency components of cover image are selected using formula ((Column + ‘t’) % ‘P’) where ‘t’ is number of bits per Byte and ‘P’ is last position level from LSB towards MSB. For example, if the ‘real part of vertical frequency’ representing values as shown in figure 6, with 8 bit representation and 32bits of information as bits stream S# = “10011001, 11100101, 10011101, 11001101”. Data is hidden in varying positions selected by hash function up to LSB+3 (P = 3) for payload of 0.5 bpB as given in figure 7, where bold bits are embedded information. While increasing the payload the same hash function may be used with different value for ‘t’ and ‘P’, such as for payload of 0.7bpB value for ‘t’ and ‘P’ become 3, and the value of ‘t’and ‘P’ taken as 4 in case of 1.0 bpB of payload.

65	78	73	30
58	78	38	32
56	73	56	35
59	70	52	39

→

01000001	01001110	01001001	00011110
00111010	01001110	00100110	00100000
00111000	01001001	00111000	00100011
00111011	01000110	00110100	00100111

Figure. 6. Frequency coefficients/binary values of 'real part of vertical frequency' sub-band

010000**01**	01001**10**0	0100**01**01	0001**0**11**1**
001110**11**	01001**01**0	0010**10**10	0010**0**00**1**
001110**01**	01001**10**1	0011**11**00	0010**0**01**1**
001110**11**	01000**00**0	0011**11**00	0010**0**11**1**

→

65	76	69	23
59	74	42	33
57	77	60	35
59	64	60	39

Figure. 7. Embedded frequency components matrix after embedding S#

The extraction technique is just the reverse of insertion.

3. RESULTS AND DISCUSSIONS

Benchmark (.pgm) images [6] are taken and applied on IAZT to formulate results. The result on ten gray scale images where representation is made-up of eight bit pixel and of dimension 512 x 512 is shown in figure 8 with secret coin of various dimensions. IAZT allow only four subbands [16], out of eight, to regenerate lossless image at destination with ideal outcome, that mean MSE zero and that of PSNR is infinity. This minimizes the energy and the bandwidth near to half.

As stated in section 2.1, on applying forward transformation in Z – domain four complex frequency coefficients are generated in the form of a + j b. On segregating real and imaginary part of forward Z transformation eight component/bands generate as shown in figure 9.b and 9.c. Out of which only four are selected to transmit over network for destination after inverse transformation. The pictorial representation of the whole process is given in figure 9.

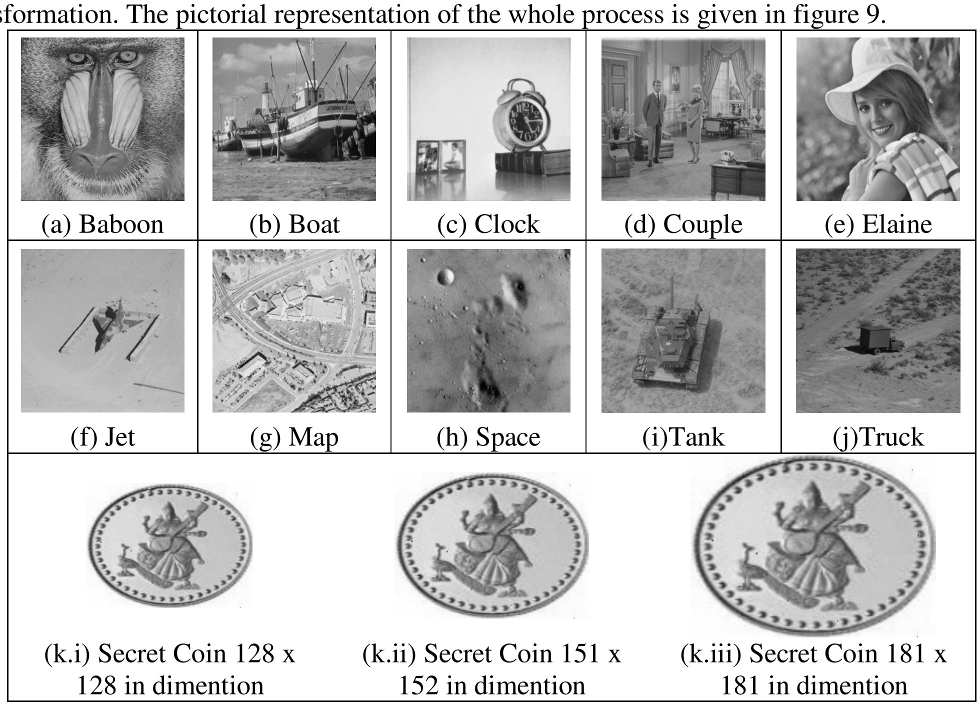

Figure. 8. Cover image of 512 x 512 dimension with secret coin image

Thus for hiding invisible watermark through IAZT maximum four bands are available as shown in figure (9.d). The overall statistical calculation between figure (9.a) and figure (9.f) such as MSE, PSNR, IF [7], UQI and SSIM [17] are calculated to know the degradation in stego-image after inverse transformation due to embedding is given in section 3.1 to 3.5. A comparative study has also been made between various existing techniques and IAZT discussed in section 3.6.

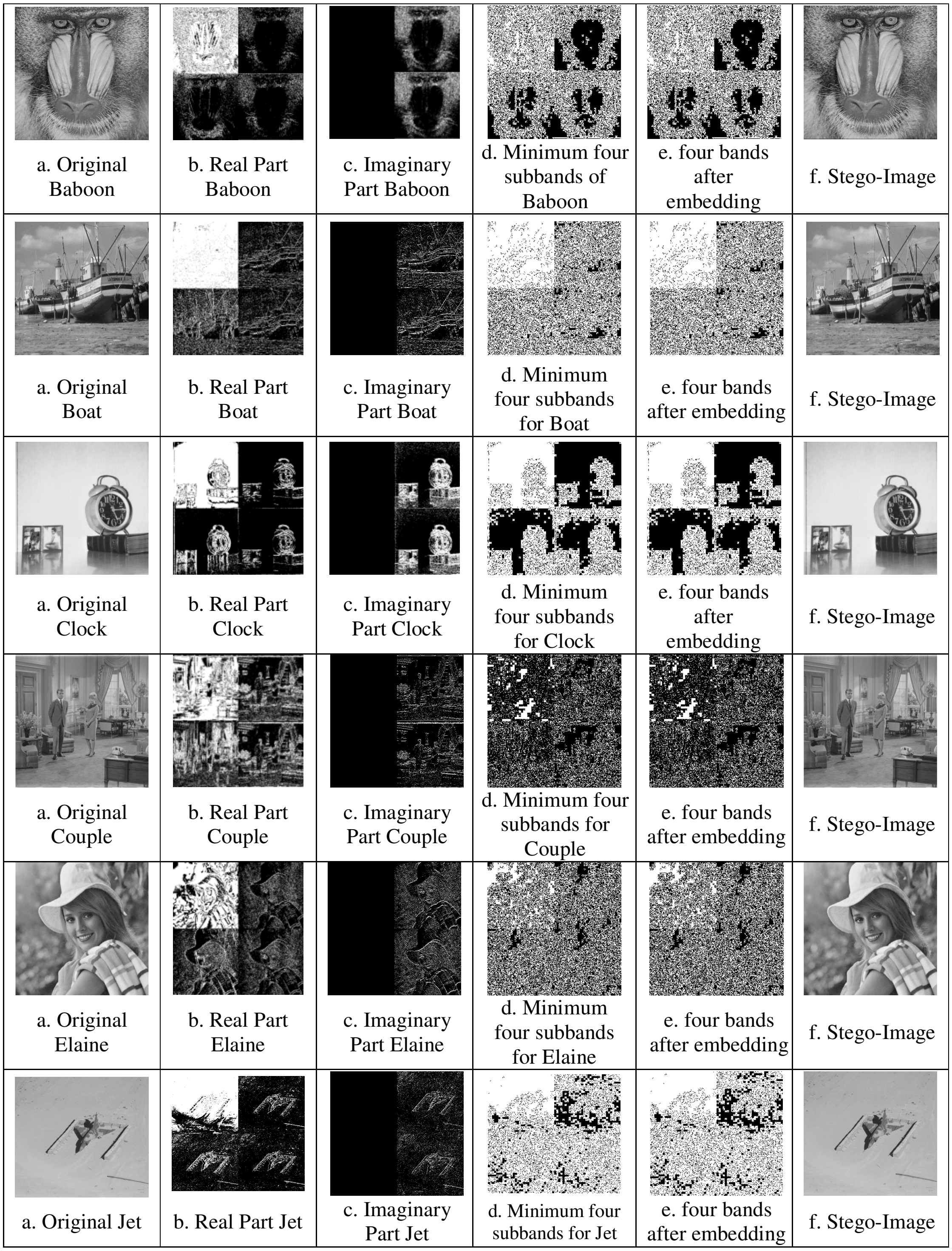

a. Original Baboon	b. Real Part Baboon	c. Imaginary Part Baboon	d. Minimum four subbands of Baboon	e. four bands after embedding	f. Stego-Image
a. Original Boat	b. Real Part Boat	c. Imaginary Part Boat	d. Minimum four subbands for Boat	e. four bands after embedding	f. Stego-Image
a. Original Clock	b. Real Part Clock	c. Imaginary Part Clock	d. Minimum four subbands for Clock	e. four bands after embedding	f. Stego-Image
a. Original Couple	b. Real Part Couple	c. Imaginary Part Couple	d. Minimum four subbands for Couple	e. four bands after embedding	f. Stego-Image
a. Original Elaine	b. Real Part Elaine	c. Imaginary Part Elaine	d. Minimum four subbands for Elaine	e. four bands after embedding	f. Stego-Image
a. Original Jet	b. Real Part Jet	c. Imaginary Part Jet	d. Minimum four subbands for Jet	e. four bands after embedding	f. Stego-Image

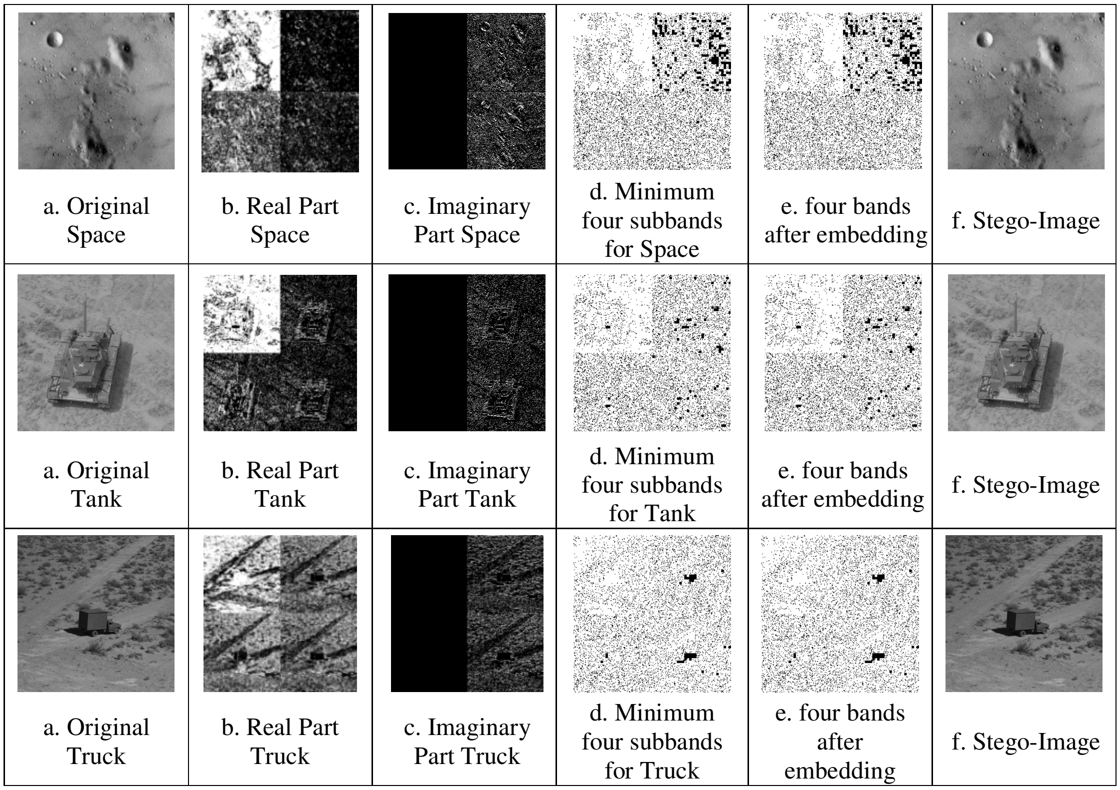

Figure. 9. Original image with its threshold image representing frequency coefficients after FZT, minimum band representation, bands after embedding and stego image after inverse Z-transform

Table 1. Statistical analysis on embedding 128 x 128 dimention secret image in vertical subband/ 'Real part of VF' band, Payload 0.5 bpB.

Cover Image 512 x 512	**MSE**	**PSNR*(dB)***	**IF**	**UQI**	**SSIM**
Baboon	0.502270	51.121433	0.999973	0.999904	0.999905
Boat	3.204308	43.073462	0.999831	0.999292	0.999302
Clock	0.459827	51.504855	0.999988	0.999948	0.999949
Couple	0.446041	51.637055	0.999973	0.999876	0.999878
Elaine	0.447857	51.619411	0.999978	0.999923	0.999924
Jet	0.457809	51.523956	0.999985	0.999661	0.999680
Map	0.446541	51.632192	0.999987	0.999899	0.999901
Space	0.446934	51.628372	0.999974	0.999787	0.999795
Tank	0.449867	51.599960	0.999975	0.999784	0.999792
Truck	0.451534	51.583896	0.999963	0.999781	0.999789
Average	***0.7312988***	***50.6924592***	***0.9999627***	***0.9997855***	***0.9997915***

Table 2. Statistical analysis on embedding 128 x 128 dimention secret image in horizontal subband/ 'Real part of HF' band from four minimum bands, Payload 0.5 bpB.

Cover Image 512 x 512	MSE	PSNR*(dB)*	IF	UQI	SSIM
Baboon	0.396255	52.151051	0.999979	0.999898	0.999899
Boat	0.405952	52.046052	0.999979	0.999910	0.999911
Clock	0.479259	51.325096	0.999987	0.999928	0.999929
Couple	0.404308	52.063677	0.999975	0.999848	0.999851
Elaine	0.404396	52.062734	0.999981	0.999908	0.999909
Jet	0.471886	51.392436	0.999985	0.999534	0.999561
Map	0.471886	51.392436	0.999985	0.999534	0.999561
Space	0.415325	51.946921	0.999976	0.999730	0.999740
Tank	0.412228	51.979433	0.999977	0.999730	0.999740
Truck	0.413258	51.968595	0.999966	0.999729	0.999739
Average	***0.4274753***	***51.8328431***	***0.999979***	***0.9997749***	***0.999784***

Table 3. Statistical analysis on embedding 128 x 128 dimention secret image in diagonal subband/ 'Imaginary part of HF' band from four minimum bands, Payload 0.5 bpB.

Cover Image 512 x 512	MSE	PSNR*(dB)*	IF	UQI	SSIM
Baboon	0.396385	52.149629	0.999979	0.999898	0.999899
Boat	0.400246	52.107537	0.999979	0.999911	0.999912
Clock	0.455513	51.545796	0.999988	0.999932	0.999932
Couple	0.402924	52.078577	0.999975	0.999848	0.999852
Elaine	0.402523	52.082896	0.999981	0.999908	0.999910
Jet	0.474091	51.372190	0.999985	0.999532	0.999559
Map	0.404316	52.063595	0.999988	0.999875	0.999877
Space	0.409069	52.012837	0.999976	0.999734	0.999744
Tank	0.414387	51.956745	0.999977	0.999728	0.999739
Truck	0.416115	51.938672	0.999966	0.999727	0.999737
Average	***0.4175569***	***51.9308474***	***0.9999794***	***0.9998093***	***0.9998161***

Table 4. Statistical analysis on embedding 151 x 152 dimention secret image in horizontal subband/'Real part of HF' band from four minimum bands, Payload 0.7 bpB.

Cover Image 512 x 512	MSE	PSNR*(dB)*	IF	UQI	SSIM
Baboon	1.378391	46.737078	0.999926	0.999634	0.999640
Boat	1.448845	46.520585	0.999924	0.999670	0.999675
Clock	2.138859	44.828982	0.999943	0.999670	0.999673
Couple	1.532902	46.275660	0.999906	0.999408	0.999421
Elaine	1.455166	46.501679	0.999930	0.999660	0.999665
Jet	1.721626	45.771415	0.999945	0.998259	0.998357
Map	1.497513	46.377098	0.999956	0.999523	0.999532

Cover Image 512 x 512	**MSE**	**PSNR*(dB)***	**IF**	**UQI**	**SSIM**
Space	1.620136	46.035288	0.999905	0.998916	0.998957
Tank	1.457527	46.494637	0.999920	0.999016	0.999053
Truck	1.473133	46.448384	0.999879	0.999006	0.999044
Average	***1.5724098***	***46.1990806***	***0.9999234***	***0.9992762***	***0.9993017***

Table 5. Statistical analysis on embedding 151 x 152 dimention secret image in diagonal subband/'Imaginary part of HF' band from four minimum bands, Payload 0.7 bpB.

Cover Image 512 x 512	**MSE**	**PSNR**	**IF**	**UQI**	**SSIM**
Baboon	1.382816	46.723159	0.999926	0.999633	0.999639
Boat	1.438732	46.551004	0.999924	0.999673	0.999677
Clock	2.067417	44.976522	0.999945	0.999681	0.999684
Couple	1.538448	46.259974	0.999905	0.999406	0.999419
Elaine	1.449154	46.519659	0.999930	0.999661	0.999666
Jet	1.713501	45.791960	0.999945	0.998267	0.998365
Map	1.490669	46.396991	0.999956	0.999526	0.999534
Space	1.526279	46.294463	0.999911	0.998979	0.999018
Tank	1.460400	46.486086	0.999920	0.999014	0.999052
Truck	1.480503	46.426710	0.999879	0.999001	0.999039
Average	***1.5547919***	***46.2426528***	***0.9999241***	***0.9992841***	***0.9993093***

Table 6. Statistical analysis on embedding 181 x 181 dimention secret image in horizontal subband/'Real part of HF' band from four minimum bands, Payload 1.0bpB.

Cover Image 512 x 512	***MSE***	***PSNR***	***IF***	**UQI**	**SSIM**
Baboon	6.068684	40.299859	0.999673	0.998384	0.998409
Boat	6.856552	39.769746	0.999639	0.998433	0.998454
Clock	10.708042	37.833703	0.999717	0.998343	0.998358
Couple	7.724094	39.252328	0.999525	0.997007	0.997073
Elaine	6.661247	39.895248	0.999678	0.998437	0.998458
Jet	9.097958	38.541365	0.999709	0.990827	0.991339
Map	7.105892	39.614617	0.999792	0.997730	0.997772
Space	8.718529	38.726372	0.999489	0.994164	0.994385
Tank	6.680252	39.882875	0.999634	0.995477	0.995649
Truck	6.877502	39.756496	0.999436	0.995347	0.995524
Average	***7.6498752***	***39.3572609***	***0.9996292***	***0.9964149***	***0.9965421***

Table 7. Statistical analysis on embedding 181 x 181 dimention secret image in horizontal subband/'Imaginary part of HF' band from four minimum bands, Payload 1.0bpB.

Cover Image 512 x 512	***MSE***	***PSNR***	***IF***	***UQI***	***SSIM***
Baboon	6.099918	40.277563	0.999672	0.998376	0.998401
Boat	6.778450	39.819500	0.999643	0.998451	0.998471
Clock	10.442543	37.942741	0.999724	0.998384	0.998398
Couple	7.720406	39.254402	0.999526	0.997008	0.997075
Elaine	6.601910	39.934108	0.999681	0.998450	0.998471
Jet	9.111351	38.534976	0.999708	0.990814	0.991326
Map	7.102764	39.616530	0.999792	0.997732	0.997773
Space	8.015533	39.091479	0.999530	0.994632	0.994835
Tank	6.672466	39.887940	0.999635	0.995482	0.995654
Truck	6.873344	39.759123	0.999437	0.995350	0.995527
Average	***7.5418685***	***39.4118362***	***0.9996348***	***0.9964679***	***0.9965931***

Table 8. Summay table of analysis based on different bands used for embedding with various Payload.

Calcula-tion	Real part of VF (0.5bpB)	Real part of HF (0.5bpB)	Imaginary part of HF (0.5bpB)	Real part of HF (0.7bpB)	Imaginary Part of HF (0.7 bpB)	Real part of HF (1.0bpB)	Imaginary part of HF (1.0bpB)
MSE	0.7312988	0.4274753	0.4175569	1.5724098	1.5547919	7.6498752	7.5418685
PSNR	50.692459	51.832843	51.930847	46.199081	46.242653	39.357261	39.411836
IF	0.9999627	0.999979	0.9999794	0.9999234	0.9999241	0.9996292	0.9996348
UQI	0.9997855	0.9997749	0.9998093	0.9992762	0.9992841	0.9964149	0.9964679
SSIM	0.9997915	0.999784	0.9998161	0.9993017	0.9993093	0.9965421	0.9965931

3.1. Error Rate (MSE)

In statistics, the mean square error or MSE [7, 17] of an estimator is one of the many ways to quantify the difference between an estimator and the true value of the quantity being estimated. The MSE represents the cumulative squared error between the embedded and the original image, the lower the value of MSE, the lower the error. In IAZT technique MSE increases with the increase in payload and with the real value coefficients toward vertical frequency. Figure 10 represent the impact on error with different bands embedded with secret information with varying payload.

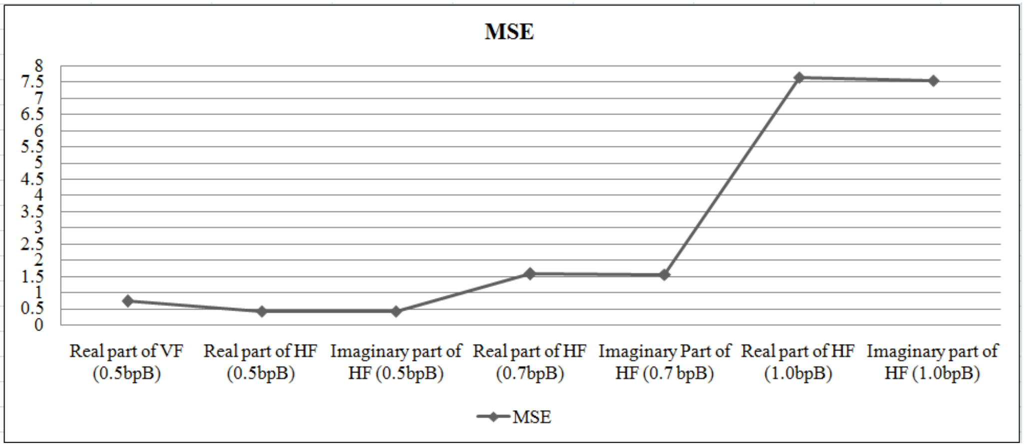

Figure. 10. Graphical representation of impact on MSE with varying bands and payload

3.2. Peak Signal to Noise Ratio (PSNR)

The peak signal-to-noise ratio, often abbreviated PSNR [7, 17], is the ratio between the maximum possible power of a signal and the power of corrupting noise that affects the fidelity of its representation PSNR is usually expressed in terms of the logarithmic decibel scale. In IAZT technique PSNR decreases with increase in payload and it also decreases while selecting bands of real value towards vertical coefficient for embedding. Figure 11 represent the impact on PSNR in dB with different bands embedded with secret information with varying payload.

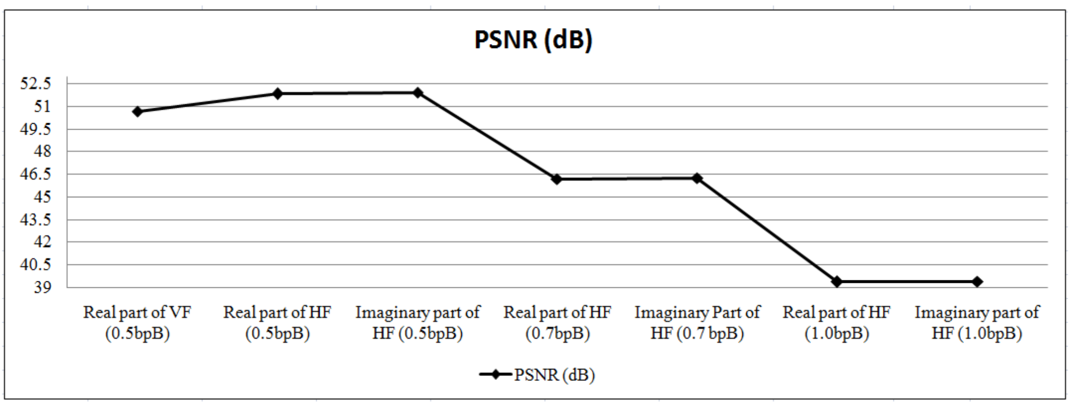

Figure. 11. Graphical representation of impact on PSNR in dB with varying bands and payload

3.3. Image fidelity (IF)

Image fidelity [7] is a parametric computation to quantify the perfectness of human visual perception. In IAZT technique IF also decreases with increase in payload and it also decreases while selecting bands of real value towards vertical coefficient for embedding. Figure 12 represent the impact on image fidelity with different bands embedded with secret information with varying payload.

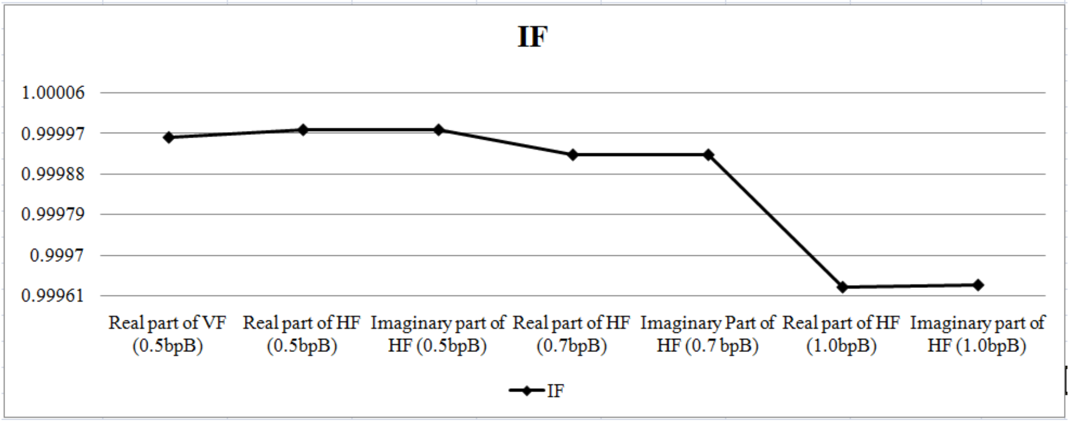

Figure. 12. Graphical representation of impact on Image fidelity with varying bands and payload

3.4. Universal Quality Image (UQI)

UQI [17] is a method to model any image distortion via a combination of three factors: loss of correlation, luminance distortion, and contrast distortion. In IAZT technique UQI index also decreases with increase in payload and it also decreases while selecting bands of real value towards vertical frequency coefficients for embedding. Figure 13 represent the impact on UQI with different bands embedded with secret information with varying payload.

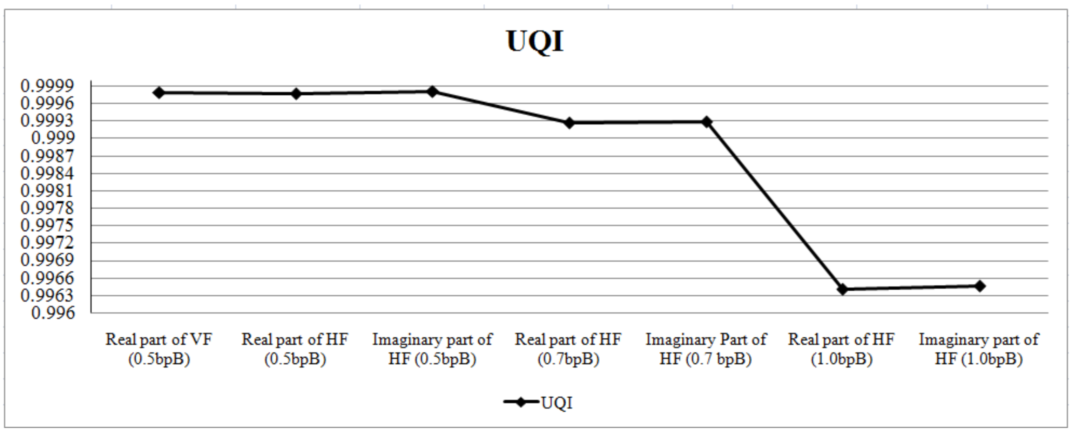

Figure. 13. Graphical representation of impact on Universal Quality Image index with varying bands and payload

3.5. Structural Similarity Index Measurement (SSIM)

Structural similarity can be obtained by comparing local patterns of pixel intensities that have been normalized for luminance and contrast. Calculation of SSIM depends on the separate calculation of luminance, contrast and structure. In IAZT SSIM also behave same as of IF or UQI. Figure 14 represent the impact on SSIM with different bands embedded with secret bits of information with varying payload.

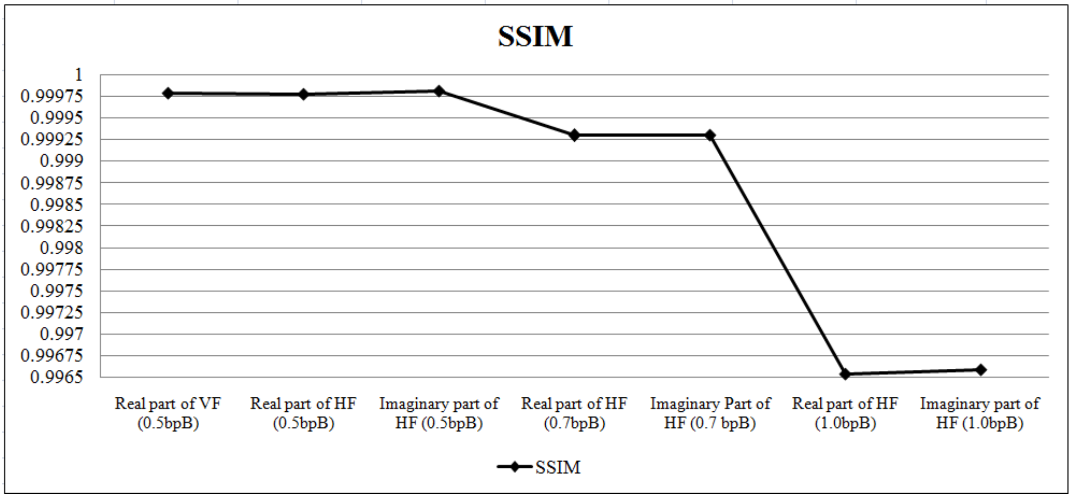

Figure. 14. Graphical representation of impact on Structural Similarity Index Measurement with varying bands and payload

3.6. Comparison of IAZT with Existing Techniques

A comparative study has been made between Li method [11], SCDFT [13], Region–Based [14], IAHTSSDCT[10], AWTDHDS[12] and SADT [15] in terms of mean square error, peak signal to noise ratio and payload (bits per Byte). Comparison is done on average of ten PGM images of figure 8, and the computation is given in table 9.

For the payload 0.5 bpB IAZT technique achieved 51.93 dB of PSNR, graphical representation of the comparison is given in figure 15.a. For 0.7 bpB PSNR become 46.24 and for 1.0bpB PSNR comes down to 39.4 shown in figure 15.b. The value obtained for PSNR in IZAT for 1.0 bpB of payload is almost optimum as compared to all other technique graphically represented in figure 15.c.

Table 9. Comparison of IAZT with existing techniques

Technique	*Capacity (bytes)*	*Size of cover image*	*bpB (Bits per bytes)*	*PSNR in dB*
Yuancheng Li's Method [11]	1089	257 * 257	0.13	28.68
SCDFT [13]	3840	512 * 512	0.12	30.10
SADCT [9]	8192	512 * 512	0.08	56.63
Region-Based [14]	16384	512 * 512	0.5	40.79
IAHTSSDCT [10]	16384	512 * 512	0.5	47.48
AWTDHDS [12]	16384	512 * 512	0.5	44.87
SAWT [8]	131072	512 * 512	1.3	36.62
SADT [15]	16384	512 * 512	0.5	49.69
SADT [15]	32768	512 * 512	1.0	46.36
IAZT	16384	512 * 512	0.5	51.93
IAZT	22952	512 * 512	0.7	46.24
IAZT	32761	512 * 512	1.0	39.41

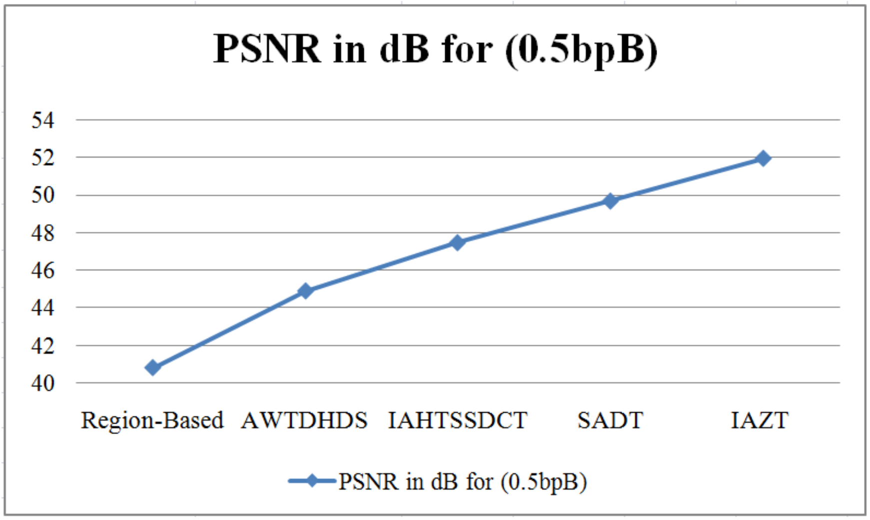

(a) Graphical representation of IAZT with existing technique on embedding 0.5 bpB of payload

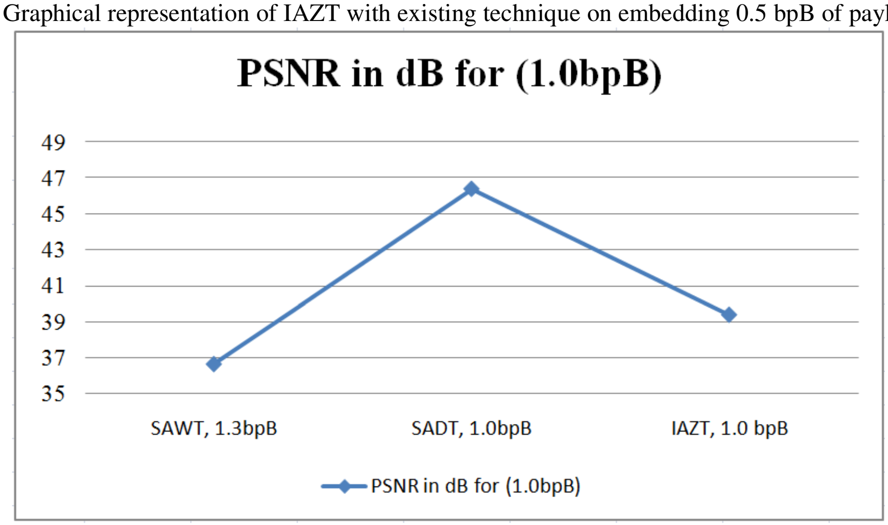

(b) Graphical representation of IAZT with existing technique on embedding 1.0 bpB of payload

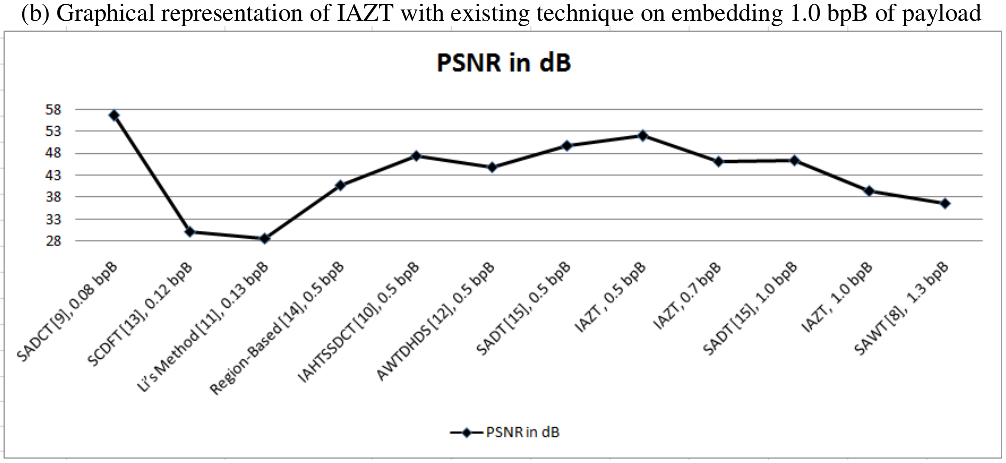

(c) Graphical representation of IAZT with existing technique for all the variations

Figure. 15. Graphical representation of comparison of IAZT with existing techniques

4. CONCLUSIONS

In this paper IAZT, the issue of image coding with minimum calculation and less complexity with invisible watermarking is achieved. IAZT also emphasis the subband minimization technique, out of eight subbands only four is enough to regenerate the image without loss this lower the energy consumption and the bandwidth too. And with the minimized four subband secret message may also be transmitted with nominal distortion in terms of fidelity and PSNR. On comparison with other standard techniques, it is observed that the proposed IAZT shows optimum performance.

ACKNOWLEDGEMENTS

The authors express deep sense of gratuity towards the Dept of CSE University of Kalyani where the computational resources are used for the work and the PURSE scheme of DST, Govt. of India.

REFERENCES

[1] Ghoshal, Nabin, and Mandal, Jyotsna Kumar, "A Novel Technique for Image Authentication in Frequency Domain Using Discrete Fourier Transformation Technique (IAFDDFTT)". Malaysian Journal of Computer Science, Vol 21 (No. 1). pp. 24-32. ISSN 0127-9084, University of Malaya, Malyasia, 2008.

[2] Madhumita Sengupta, J. K. Mandal, "Authentication of Images through Non Convoluted DCT (AINCDCT)", first International Conference on Communication and Industrial Application (ICCIA 2011), Dec, 26-28, 2011, IEEE, pp- 1-4, DOI: 10.1109/ICCIndA.2011.6146672.

[3] Madhumita Sengupta, J. K. Mandal, Nabin Ghoshal, "An authetication technique in frequency domain through wavelet transform (ATFDWT), Advances in Modelling Signal Processing and Pattern Recognition(AMSE), vol-54, Issue 2, 2011, Published Journal:2011-Vol.54No1-2.

[4] J. K. Mandal, Madhumita Sengupta, "Steganographic Technique Based on Minimum Deviation of Fidelity (STMDF)", IEEE, Second International Conference on Emerging Applications of Information Technology (EAIT 2011), Print ISBN: 978-1-4244-9683-9, DOI: 10.1109/EAIT.2011.24, Issue Date: 19-20 Feb. 2011 pp- 298 - 301.

[5] J. K. Mandal, Madhumita Sengupta, "Authentication /Secret Message Transformation Through Wavelet Transform based Subband Image Coding (WTSIC)", IEEE, ISED- 2010, pp 225-229, ISBN 978-0-7695-4294-2, Bhubaneswar, India, Print ISBN: 978-1-4244-8979-4, Dec, 20th -22nd, 2010, DOI 10.1109/ISED.2010.50.

[6] Allan G. Weber, The USC-SIPI Image Database: Version 5, Original release: October 1997, Signal and Image Processing Institute, University of Southern California, Department of Electrical Engineering. http://sipi.usc.edu/database/ (accessed on 25th January, 2012).

[7] Kutter M , Petitcolas F A P. A fair benchmark for image watermarking systems, Electronic Imaging 99. Security and Watermarking of Multimedia Contents. vol. 3657. Sans Jose, CA, USA. January 1999. The International Society for Optical Engineering. pp 226-239.

[8] Madhumita Sengupta, J.K. Mandal, "Self Authentication of Color image through Wavelet Transformation Technique (SAWT)", pp- 151-154, ISBN 93-80813-01-5, ICCS 2010.

[9] Madhumita Sengupta, J. K. Mandal, "Self Authentication of Color Images through Discrete Cosine Transformation (SADCT)", IEEE catalog no: CFP1122P-CDR, ICRTIT, Anna University, Chennai, ISBN No-: 978-1-4577-0589-2, 3rd-5th June 2011.

[10] Madhumita Sengupta, J. K. Mandal "Image Authentication using Hough Transform generated Self Signature in DCT based Frequency Domain (IAHTSSDCT)", IEEE, ISED- 2011, Kochi, Kerala, pp- 324-328, DOI 10.1109/ISED.2011.43, 2011.

[11] Li Yuancheng, Xiaolei Wang, "A watermarking method combined with Radon transform and 2D-wavelet transform", IEEE, Proceedings of the 7th World Congress on Intelligent Control and Automation, June 25 - 27, Chongqing, China, 2008.

[12] Madhumita Sengupta, J. K. Mandal, "Authentication in Wavelet Transform Domain through Hough Domain Signature (AWTDHDS)" UGC-Sponsored National Symposium on Emerging Trends in Computer Science (ETCS 2012), ISBN number 978-81-921808-2-3, pp 61-65, 2012.

[13] T. T. Tsui, X. –P. Zhang, and D. Androutsos, Color Image Watermarking Usimg Multidimensional Fourier Transformation, IEEE Trans. on Info. Forensics and Security, vol. 3, no. 1, pp. 16-28, 2008.

[14] A. Nikolaidis, I. Pitas, "Region-Based Image Watermarking", IEEE Transactions on Image Processing, Vol. 10, NO. 11, pp. 1721-1740, November 2001.

[15] Madhumita Sengupta and J. K. Mandal, "Self Authentication of image through Daubechies Transform technique (SADT)", First International Conference on Intelligent Infrastructure, CSI-2012, 47th Annual National Convention, Organised by: Computer Society of India, Kolkata Chapter, Proceedings published by Tata McGraw Hill Education Private Limited, ISBN(13):978-1-25-906170-7, ISBN(10): 1-25-906170-1, pp- 249-252, December, 2012.

[16] Madhumita Sengupta and J. K. Mandal, "Image coding through Z-Transform with low Energy and Bandwidth (IZEB)", The Third International Conference on Computer Science and Information Technology (CCSIT- 2013), Bangalore, India, 18-20, Feb (2013), Paper ID 182.

[17] Zhou Wang, Alan Conrad Bovik, et. al. "Image Quality Assessment: From Error Visibility to Structural Similarity", IEEE Transactions on Image Processing, Vol. 13, No. 4, pp 600- 612, April 2004.

AUTHORS

Madhumita Sengupta

M. Tech (CSE, University of Kalyani, 2010), pursuing Ph.D. as University Research Scholar (University of Kalyani), in the field of Transform domain based Image Processing, Steganography. Total number of publications 14.

Prof. Jyotsna Kumar Mandal

M. Tech.(Computer Science, University of Calcutta), Ph.D.(Engg., Jadavpur University) in the field of Data Compression and Error Correction Techniques, Professor in Computer Science and Engineering, University of Kalyani, India. Life Member of Computer Society of India since 1992 and life member of cryptology Research Society of India. Ex-Dean Faculty of Engineering, Teachnology & Management, work ing in the field of Network Security, Steganography, Remote Sensing & GIS Application, Image Processing. 26 years of teaching and research experiences. Nine Scholars awarded Ph.D. one submitted and eight are pursuing. Total number of publications is more than two hundred eight one in addition of publication of five books from LAP Lambert, Germany.